ELSEVIER

International Journal of Refrigeration 25 (2002) 1025–1033

REVUE INTERNATIONALE DU FROID
INTERNATIONAL JOURNAL OF
refrigeration

www.elsevier.com/locate/ijrefrig

The electro-adsorption chiller: a miniaturized cooling cycle with applications to micro-electronics

Jeffrey M. Gordon[a,b,*], K.C. Ng[c], H.T. Chua[c,1], A. Chakraborty[c]

[a]*Department of Solar Energy and Environmental Physics, Jacob Blaustein Institute for Desert Research, Ben-Gurion University of the Negev, Sede Boqer Campus 84990, Israel*
[b]*The Pearlstone Center for Aeronautical Engineering Studies, Department of Mechanical Engineering, Ben-Gurion University of the Negev, Beersheva 84105, Israel*
[c]*Department of Mechanical Engineering, National University of Singapore, 10 Kent Ridge Crescent, Singapore 119260, Singapore*

Received 23 November 2001; received in revised form 11 March 2002; accepted 7 May 2002

Abstract

A novel modular and miniature chiller is proposed that symbiotically combines adsorption and thermoelectric cooling devices. The seemingly low efficiency of each cycle individually is overcome by an amalgamation with the other. This electro-adsorption chiller incorporates solely existing technologies. It can attain large cooling densities at high efficiency, yet is free of moving parts and comprises harmless materials. The governing physical processes are primarily surface rather than bulk effects, or involve electron rather than fluid flow. This insensitivity to scale creates promising applications in cooling personal computers and other microelectronic appliances.

Keywords: Chiller; Thermoelectricity; Adsorption system; Hybrid system; Miniaturization; Application; Electronics

Refroidisseur thermoélectrique et à adsorption : cycle de refroidissement miniaturisé avec applications en microélectronique

Mots clés : Refroidisseur ; Thermoélectricité ; Système à adsorption ; Système mixte ; Miniaturisation ; Application ; Électronique

1. Introduction

A central challenge in cooling science today is the development of miniaturized chillers that are: (1) compact; (2) (nearly) free of moving parts; (3) efficient in converting input to cooling power; (4) capable of high cooling densities (W cm^{-2}); and (5) free of toxic and environmentally-harmful substances.

Why not simply try to design scaled-down versions of conventional mechanical (vapor-compression) or absorption chillers [1]? The answer lies in the scale dependence for both (a) the governing heat and mass transfer processes, and (b) the principal mechanical components. The primary irreversibilities in conventional chillers are bulk effects: fluid friction, mass transfer in solutions, gas expansion, etc. [1]. These irreversibilities increase dramatically as systems are miniaturized due to

* Corresponding author. Tel.: +972-8-659-6923; fax: +972-8-659-6921.
E-mail addresses: jeff@menix.bgu.ac.il (J.M. Gordon), engcht@nus.edu.sg (H.T. Chua), mpengkc@nus.edu.sg (K.C. Ng).
[1] Bachelor of Technology Programme, Faculty of Engineering, National University of Singapore, 10 Kent Ridge Crescent, Singapore 119260, Singapore.

0140-7007/02/$20.00
PII: S0140-7007(02)00026-9

Nomenclature

A	cross-sectional area
c	specific heat
COP	coefficient of performance {(cooling rate produced)/(input power)}
h	specific enthalpy
I	electrical current
L	length of thermoelectric element
M	mass
N	number of thermoelectric elements
p	pressure
P_{in}	electrical input power
q	extent of adsorption/desorption
Q	heat transfer rate
t	time
t_{switch}	switching time between sorption beds
UA	thermal conductance
V	voltage
x	position (length coordinate) along the thermoelectric
α	Seebeck coefficient
δ	switch control
ΔH_{ads}	heat of adsorption
γ	overall control
λ	thermal conductivity
ρ_{dens}	thermoelectric density
ρ_{elec}	electrical resistivity
σ	switch control
τ	cycle time of the electro-adsorption chiller

Subscripts

ads	adsorber/adsorption
air	air cooling the condenser
bed,i	sorption bed i
cond	condenser
connect	substrate and plate that connect the bed and thermoelectric
des	desorber/desorption
evap	evaporator
f	fluid (liquid) phase
g	vapor (gas) phase
hx	heat exchanger
H	hot junction
junc	(hot or cold) junction
load	cooling load surface
L	cold junction
net	net or overall performance
sg	silica gel
TE	thermoelectric

Superscripts

refr	refrigerant

the combination of (a) an unfavourable ratio of surface area to volume, and (b) the functional dependencies of dissipative mechanisms on scale. Consequently, chiller efficiency is reduced to unsatisfactorily low levels. The compressors that lie at the heart of mechanical chillers cannot be miniaturized without a sizable loss of efficiency. The scaling down of fluid pumps and fluid control systems is comparably disfavored. (Recent efforts to miniaturize absorption chillers with micro-channel generators, absorbers and heat exchangers are reported in [2].)

Thermoelectric chillers [3–5] (Fig. 1) satisfy the requirements of compactness, the absence of moving parts, and an insensitivity to scale (since energy transfers derive from electron flows), but suffer from inherently low coefficient of performance (COP=[cooling power produced]/[input power]), typically in the range of 0.1–0.4 for the temperatures characteristic of many microelectronic applications, where Bi_2Te_3 is the current material of choice.

Adsorption chillers [6] (Fig. 2) might appear to offer an additional option, because adsorption and desorption are primarily surface, rather than bulk, processes. A refrigerant such as water is exothermically adsorbed, and endothermically desorbed, from the porous surfaces of a bed material such as silica gel. The necessary energy transfers are supplied by heat exchangers to separate reservoirs.

Commercially-available adsorbent-adsorbate pairs include silica gel-water, zeolite-water, activated carbon-methanol, and silica gel-methanol. Silica gel-water has been the preferred pair in adsorption chiller development owing to (a) silica gel's comparatively large uptake capacity for water; (b) the high heat of vaporization of water; (c) the relatively low temperatures for desorption; and (d) the harmless nature of the chemicals.

However, the inappropriateness of miniaturized adsorption cycles lies in (a) inherently low COPs (in the range of 0.1–0.6 for typical air-conditioning uses), and (b) the problematic nature of scaling down the fluid pumps, coolant loops and fluid pumps without substantial performance losses. The intrinsically low COP is related to (1) small temperature differences among the reservoirs, and (2) the requirement of batchwise operation.

We will explain how a unique union of the adsorption and thermoelectric chillers can produce a device that fulfils the aims noted at the beginning of this section, with the added virtues of: (a) scale independence, which permits chiller miniaturization and system compactness; (b) no coolant loops, which eliminates fluid pumps and fluid control systems; (c) production from existing

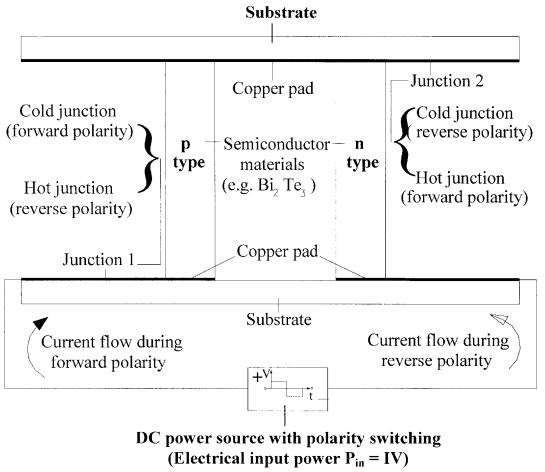

Fig. 1. Thermoelectric chiller schematic. The semiconductor is doped to produce an excess of electrons in one element (n-type) and a dearth of electrons in the other (p-type). When a voltage V is applied, and an electrical current I passes through two dissimilar thermoelectric materials (electrical input power $P_{in} = IV$), one element heats up to temperature T_H while the other cools to T_L, referred to as the Peltier effect. Thermoelectric chillers are usually built with multiple couples that are connected electrically in series and thermally in parallel. The option of polarity switching for the DC power source is shown, in anticipation of such a control in Section 2.1.

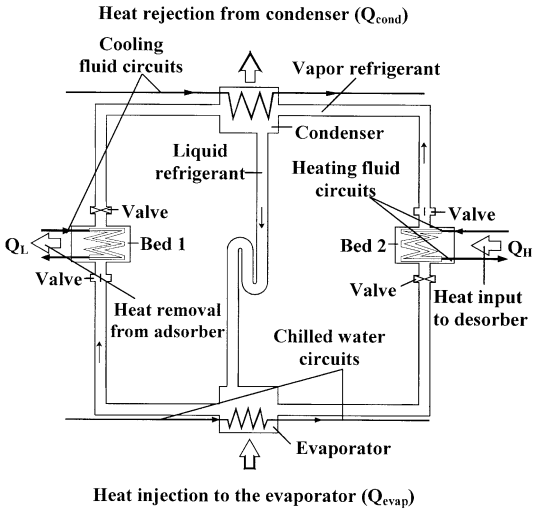

Fig. 2. Schematic of an adsorption chiller. The cooling cycle is driven by heat input at the desorber where refrigerant is driven out of the adsorbent bed and heated. Refrigerant is then condensed, followed by refluxing to the evaporator via a pressure-reduction valve, and refrigerant adsorption in the heat-rejecting adsorber bed. Due to the relatively long times required for saturation in adsorption and desorption, batch processing is required. Valves at the entrance and exit of the adsorber and desorber restrict refrigerant flow as needed, i.e., to ensure separation of the two autonomous periods of (1) desorption/adsorption, and (2) switching between the beds.

technologies (namely, its realization is not contingent upon the development of new materials or unfamiliar components); and (d) modularity, which offers the possibility of assembling prescribed cooling rates from a number of miniaturized cooling units.

2. The electro-adsorption chiller cycle

2.1. The thermodynamic cycle

We are proposing cascading the thermoelectric and adsorption chiller cycles [7] as illustrated in Fig. 3. The thermoelectric junctions are separately attached to the two beds of the adsorption chiller in a thermally conductive but electrically non-conductive manner. The cold junction absorbs thermal power in driving the adsorption of refrigerant (e.g., water) onto the adsorbent (e.g., silica gel). The hot junction emits thermal power that drives the desorption of refrigerant from the adsorbent. During the heating and cooling of the beds, small on/off valves ensure that no refrigerant flows into or out of the beds.

After adequate heat transfer is effected, a timed controller activates the opening of the valves. Heated refrigerant from the desorber is released to a condenser for heat rejection to the environment. Vaporized refrig-

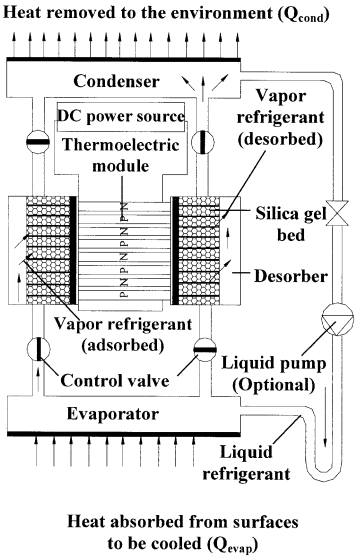

Fig. 3. Schematic showing the principal components and energy flows of the electro-adsorption chiller. The optional circulation pump is intended as a micro-electronic mechanical pump for highly miniaturized chillers, where condensate return action solely via a U-tube might be acutely sensitive to orientation changes.

erant is fed to the adsorber from the evaporator which in turn cools the load of interest.

In order to complete the cooling cycle, the roles of adsorber and desorber must be reversed. In conventional adsorption chillers, this is accomplished by switching the flow of coolant water to the two beds with forced-circulation pumps and valves. In the electro-adsorption cooling cycle, bed switching is performed simply by reversing the polarity of the voltage V applied to the thermoelectric (as in Fig. 1). What was formerly the cold junction becomes the hot junction and vice versa. The cycle is now complete. The heating and cooling of the two beds repeat, along with the flow of refrigerant to and from the condenser, evaporator, adsorber and desorber.

The thermal bottleneck in the cycle is boiling heat transfer in the evaporator—a modular component, the capability of which essentially dictates the achievable cooling density of the chiller. We will examine the performance of the electro-adsorption chiller for boiling heat transfer rates that correspond to state-of-the art pool-boiling evaporators (up to about 10 W cm^{-2}). In principle, ultra-high boiling heat transfer rates are attainable (in excess of 100 W cm^{-2}) with methods such as spray jet injection. The absence of measurements at the temperatures and pressures of the cooling regimes considered here militated against generating non-rigorous projections for such optimistic scenarios in this study, but will be incorporated as such data become available.

2.2. *Chiller* COP

The cycle-average COP of the electro-adsorption chiller, COP_{net}, can be expressed in terms of the cycle-average COPs of the individual adsorption (subscript $_{ads}$) and thermoelectric (subscript $_{TE}$) chillers by considering the overall energy flows (with all energy flows defined as positive). Note, however, that COP_{ads} is a complicated function of COP_{TE} via the dynamics of the combined cycle (see the Appendix).

Referring to Fig. 3, we define the COPs of the individual components as the nominal cycle-average cooling rate produced relative to the particular (electrical or thermal) cycle-average power input:

$$COP_{TE} = Q_L/P_{in} \tag{1}$$

$$\mathrm{COP_{ads}} = \mathrm{Q_{evap}}/Q_H \tag{2}$$

where Q_{evap} denotes the cycle-average cooling rate of the overall device, i.e. the rate of heat extraction at the evaporator. The cycle-average values of the thermal power absorbed at the cold junction Q_L that drives refrigerant adsorption, as well as the thermal power rejected at the hot junction Q_H that drives refrigerant desorption, are indicated in Fig. 2 for the adsorption cycle. They are not indicated in Fig. 3 in order to avoid ambiguities associated with the polarity switching.

COP_{ads} can reach (and even exceed) 1.0 as a consequence of the heat regeneration between the sorption beds, which derives from the thermoelectric effect. In contrast, COP_{TE} will fall below commonly observed thermoelectric COP values due primarily to losses associated with the large thermal lift, and secondarily to the switching process.

From the first law of thermodynamics

$$P_{in} = Q_H - Q_L \tag{3}$$

so that

$$COP_{net} = Q_{evap}/P_{in} = COP_{ads}\,(1 + COP_{TE}). \tag{4}$$

COP_{TE} and COP_{ads} are not equivalent, but are used consistently in the derivation of COP_{net}. A comparison between COP_{net} and the COP of conventional vapor-compression chillers is inappropriate because of the severe difficulty of miniaturizing the latter, which is the central thrust of this paper.

3. Device performance and simulation results

3.1. *Modeling assumptions*

The equations adopted here for the time-dependent behavior of the chiller components and their mutual interactions have been derived and validated in previous studies

(a) thermoelectric behavior, in [3]
(b) adsorption and desorption, in [6]
(c) heat exchanger dynamics, in [6],

and are summarized in the Appendix and Table 1. We have solved the complete set of coupled energy and mass transfer equations numerically to yield predictions of the key performance variables of the electro-adsorption chiller, as well as their sensitivity to several practical controls.

We adopt a cooling density of 10 W cm^{-2}, and then simulate how chiller performance variables (such as COP_{net}, cooling load surface temperature T_{load}, evaporator temperature T_{evap}, and electrical current) change with the principal control variables.

Parameters for a nominal reference system relative to which our sensitivity studies will be performed are tabulated in Table 1. They typify the size and cooling rates of typical micro-electronic cooling problems. The heat exchanger sizes are commensurate with compact units.

The maximum tolerance temperatures (for T_{load}) of computer and other micro-electronic processing units are typically above the design values chosen in the examples

Table 1
Component parameter values and material properties for a nominal reference system

Property or parameter	Value or descriptive equation
Thermoelectric (Bi_2Te_3)	
Electrical resistivity	$\rho_{elec} = (5.112 \times 10^{-6}) + (8.17 \times 10^{-9}(T_H + T_L)) + (1.567 \times 10^{-11}(T_H + T_L)^2)$ ohm-m
Thermal conductivity	$\lambda = 6.261 - (1.389 \times 10^{-2}(T_H + T_L)) + (1.033 \times 10^{-5}(T_H + T_L)^2)$ W m^{-1} K^{-1}
Seebeck coefficient	$\alpha = (2.222 \times 10^{-5}) + (4.653 \times 10^{-7}(T_H + T_L)) - (2.376 \times 10^{-10}(T_H + T_L)^2)$ V K^{-1}
Specific heat	$c_{TE} = 544$ J kg^{-1} K^{-1}
Density	$\rho_{dens} = 7.2 \times 10^{-3}$ kg m^{-3}
Cross-sectional area per element	$A_{TE} = 5 \times 10^{-3}$ m^2
Element length	$L = 5 \times 10^{-3}$ m
Number of couples	$N = 30$
Terminal voltage	$V = 0.15$ volt per element
Adsorber and desorber beds	
Thermal capacitance of the Cu substrate and ceramic plate that connect the bed and the thermoelectric	$(Mc)_{connect} = 1.782$ J K^{-1}
Kinetics for extent of adsorption q (kg of water relative to kg of silica gel)	$\frac{dq(t)}{dt} = \frac{D\exp\left(\frac{-E_a}{RT}\right)}{r^2}(q^* - q(t))$
Isotherm for water uptake at saturation q^* as a function of pressure p (R = gas constant)	$q^* = \frac{K_p \exp\left(\frac{\Delta H_{ads}}{RT}\right)}{\left[1 + \left\{(Kp/q_m)\exp\left(\frac{\Delta H_{ads}}{RT}\right)\right\}^{\beta}\right]^{1/\beta}}$
Monolayer capacity	$q_m = 0.4$ (kg water) (kg silica gel)$^{-1}$ (for type A silica gel)
Kinetic constant	$D = 3.81 \times 10^{-3}$ m^2 s^{-1}
Activation energy	$E_a = 4.2 \times 10^{-4}$ J mol^{-1}
Silica gel average radius	$r = 1.7 \times 10^{-4}$ m
Pre-exponential constant	$K = 4.65 \times 10^{-10}$ (kg water) (kg silica gel)$^{-1}$ Pa^{-1}
Isosteric heat of adsorption	$\Delta H_{ads} = 2.71 \times 10^6$ J kg^{-1}
Isotherm equation exponent	$\beta = 10$ (for type A silica gel)
Bed heat transfer area	1.2×10^{-3} m^2
Silica gel specific heat	$c_{sg} = 9.24 \times 102$ J kg^{-1} K^{-1}
Mass of silica gel	$M_{sg} = 2 \times 10^{-3}$ kg
Mass of heat exchanger	$M_{hx} = 2.5 \times 10^{-2}$ kg
Condenser	
Heat transfer area	$A_{cond} = 1.0 \times 10^{-3}$ m^2
Specific heat	$c_{cond} = 9.03 \times 10^2$ J kg^{-1} K^{-1}
Mass	$M_{cond} = 2.01 \times 10^{-2}$ kg
Heat transfer coefficient	$U_{cond} = 9.00 \times 102$ W m^{-2} K^{-1}
Maximum refrigerant mass	$M_{cond}^{ref,\ max} = 1.284 \times 10^{-3}$ kg
Evaporator	
Heat transfer area	$A_{evap} = 2.0 \times 10^{-4}$ m^2
Specific heat	$c_{evap} = 3.83 \times 10^2$ J kg^{-1} K^{-1}
Mass	$M_{evap} = 5.1 \times 10^{-3}$ kg
Heat transfer coefficient	$U_{evap} = 4.00 \times 10^3$ W m^{-2} K^{-1}
Cooling density	10 W cm^{-2}
Initial refrigerant mass	6.0×10^{-3} kg

below. The lower and highly desirable temperature regime selected for our design studies corresponds to enhanced performance of the PC or micro-electronic device (e.g., computational speed and lifetime), and sharpens the contrast with micro-thermosyphon and micro-heat-pipe heat rejection units with micro-scale heat exchangers [8], which by their very nature cannot cool below the temperature in the immediate vicinity of the cooling load.

The thermoelectric is driven at a constant applied DC voltage (but with the change in polarity explained above). The time-varying electrical current in the thermoelectric changes continuously in accordance with the

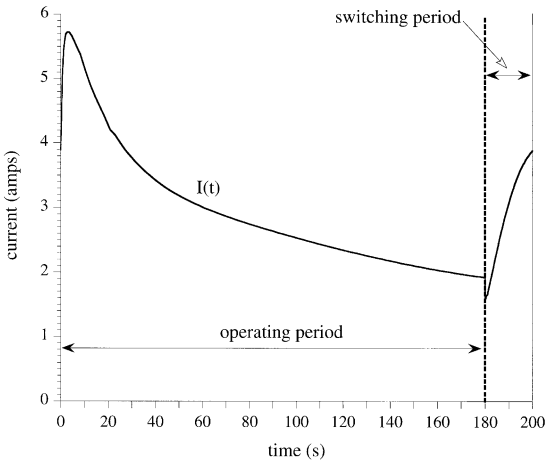

Fig. 4. The time evolution of input current during one chiller cycle at steady state. Cycle time = 200 s. Switching time = 20 s.

governing energy balance equations, as illustrated in Fig. 4.

3.2. Control variables

We consider several variables with respect to which chiller performance can be optimized:

(1) The number of thermoelectric elements N and their geometric factor (the latter being the ratio of cross-sectional area to length A_{TE}/L). The voltage (and hence the input power) is proportional to N. T_{evap} (and hence T_{load}) decreases as N increases. COP_{TE} improves as the geometric factor is lowered, at least to the limit at which manufacturers provide thermoelectric elements. Accordingly, we have used the lowest commercially-available geometric factor of 1.0 mm.
(2) The switching time between sorption beds t_{switch}. When t_{switch} is too long, T_{evap} grows excessive. At too short a t_{switch}, the adsorber has insufficient time to cool, so warm adsorbate desorbs into the evaporator (hence raising T_{evap}).
(3) The cycle time τ. For too short a cycle time, the sorption beds have insufficient time to respond (i.e., to saturate). Furthermore, the beds will consume excessive thermal power due to frequent cycling. Consequently, T_{evap} will be large. At very long τ, T_{evap} will increase with τ because the adsorbent saturates in less than the allotted time.

3.3. Chiller dynamics and performance

Fig. 5 illustrates the time evolution of the chiller's chief temperature indicators, from the initial start-up transient through cyclic steady-state. The time to reach

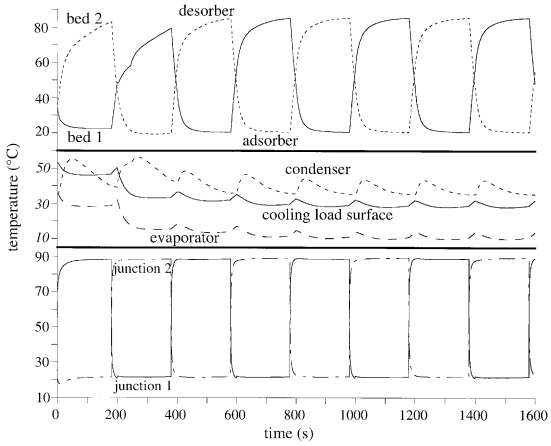

Fig. 5. Temperatures of the principal components as functions of time from initial start-up through cyclic steady-state. Cycle time = 200 s and switching time = 20 s. (a) Refrigerant in the two beds (alternating as adsorber and desorber). (b) Refrigerant in the condenser and evaporator, as well as the cooling load surface. (c) The two thermoelectric junctions (alternating hot and cold).

cyclic steady-state may be long relative to conventional chillers, but substantial cooling power is produced even during the early stages. Should more cooling power be required immediately after start-up, one could either (a) increase the input voltage, or (b) shorten the cycle time (although both measures would decrease COP_{net}). Also, despite the polarity switch, the rate of change of thermoelectric temperature remains well below typical manufacturer-specified maximum values of about 1 K s^{-1}.

Fig. 6 plots COP, T_{load} and T_{evap} against N, at the cycle times that minimize T_{evap} for each value of N. Our simulation treats the interface between the thermoelectric and the sorption beds (as well as the sorption beds themselves) as isothermal—an approximation that cannot remain realistic when N is close to unity. We

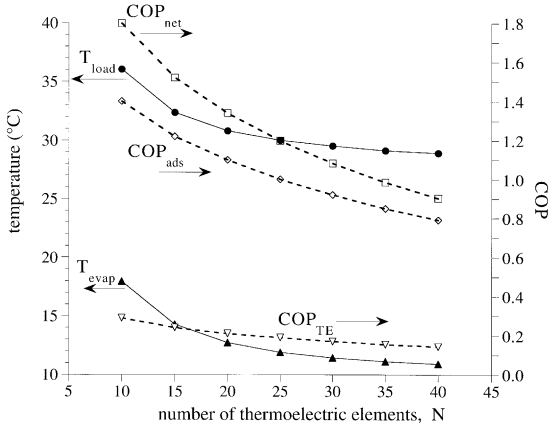

Fig. 6. T_{load}, T_{evap}, COP_{net}, COP_{TE} and COP_{ads} as functions of the number of thermoelectric elements N.

have therefore limited our configurations to $N \geqslant 10$, which is comfortably within the range of validity of the isothermal approximation. Accordingly, the curves in Fig. 6 should not be extrapolated to much lower values of N.

We chose $N = 30$—at which $COP_{net} = 1.08$—as a reference value even though COP_{net} reaches 1.8 at $N = 10$. The reason becomes apparent from Fig. 6, in conjunction with the observation that microprocessor performance is heightened at lower evaporator temperatures.

Fig. 7 shows COP_{net}, T_{load} and T_{evap} as functions of τ. For a given maximum T_{load}, the pronounced variation of T_{evap} with τ constrains both V and N (as evidenced by the results graphed in Fig. 6). Beyond the trends already anticipated above, we observe that COP_{net} reaches a limiting value at long τ because in this limit

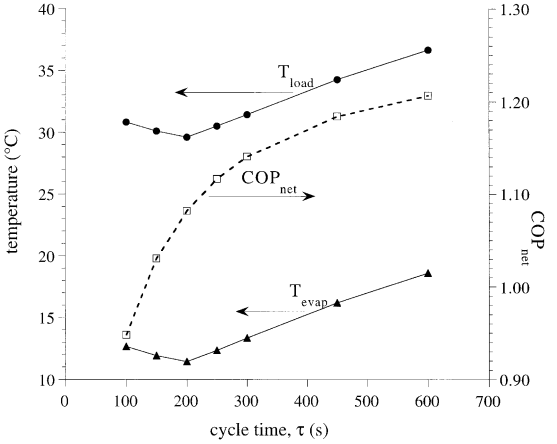

Fig. 7. COP_{net}, T_{load} and T_{evap} as functions of cycle time τ.

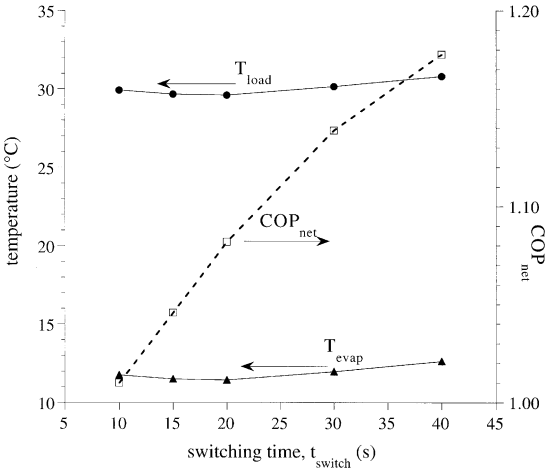

Fig. 8. T_{load}, T_{evap} and COP_{net} as functions of switching time for cycle time $\tau = 200$ s.

the impact of the thermoelectric transient grows negligible. COP_{net} can be expressed as

$$COP_{net} = \frac{\tau Q_{evap}}{\int_0^t I(t) V \mathrm{d}t}. \quad (5)$$

At long τ, $I(t)$ becomes constant (i.e., roughly time-independent), and $COP_{net} = Q_{evap}/(I\,V)$, independent of τ.

Fig. 8 portrays device optimization with respect to t_{switch} at $\tau = 200$ s, and quantifies the observations noted above regarding exceedingly long or short cycle times. Beyond the thermodynamic performance variations, there is the deleterious effect of excessive swings in T_{load} when t_{switch} is too short *or* too long.

Ultra-high cooling densities in excess of 100 W cm^{-2} are possible with spray jet-injection units, e.g., micro-electronic mechanical pumps with explosive boiling pumping action [9,10]. This technology, originally developed for ink-jet printers [11], retains the virtue of no moving parts and should be readily adaptable for use in electro-adsorption chillers (as well as other micro-cooling devices). Due to the dearth of experimental data for the conditions particular to the cooling system proposed here, we have abstained from venturing potentially imprecise estimates of cooling performance.

4. Discussion

The electro-adsorption chiller constitutes a new type of scalable, modular and efficient cooling device that overcomes the inherently low COP of the individual thermoelectric and adsorption cycles, and permits the elimination of fluid pumps, coolant loops, mechanical systems, and fluid controls that would ordinarily be problematic in the miniaturization of conventional chillers. There are essentially no moving parts (except for the small condenser fan that in any event forms an integral part of many micro-cooling units, plus the micro-valves that open and close access to the sorption beds).

The mechanically-pumped coolant loops needed to switch the heating and cooling fluid between the desorber and adsorber beds of the conventional adsorption chiller are replaced by electron flow in the thermoelectric. The switching of adsorber and desorber is effected simply by alternating the polarity of the electrical input to the thermoelectric.

The electro-adsorption chiller embodies a combined regenerative thermodynamic cycle. Heat that would normally be rejected to the environment by the thermoelectric is recovered to drive refrigerant desorption in the adsorption chiller. And heat that would ordinarily be rejected by the adsorber to the environment is regenerated by the thermoelectric at its cold junction.

COP_{ads} here is far larger than in conventional adsorption chillers (because of the regeneration). The

isolated COP_{TE} may not be superior to that of stand-alone thermoelectric chillers; but the essential functions of the thermoelectric here are (a) replacing complicated fluid pumps and piping that would ordinarily preclude miniaturization; and (b) regeneration. Furthermore, there is no competition between COP_{ads} and COP_{TE} in aiming for high COP_{net} values. Namely, control variables that raise one also increase the other, as illustrated in Fig. 6.

A number of modular micro-cooling units suitable for micro-electronic devices and spot cooling applications could readily be assembled together toward accommodating greater cooling demands. The multi-sorption-bed configuration in such a modular assembly would actually improve the quality of cooling since swings in T_{evap} would be moderated significantly [6]. For micro-electronic cooling applications, compared to existing solutions, the electro-adsorption chiller can offer significantly lower temperatures at elevated efficiency (COP).

For cooling load temperatures near ambient, e.g., up to around 35 °C, the electro-adsorption chiller also has potential uses in the cooling of machine surfaces at high heat flux. Conventional cooling methods such as thermospyhon or convective air cooling, while functionable, cannot attain comparable cooling densities of 10 W cm^{-2}.

The electro-adsorption chiller is still a proposal rather than an experimental realization. However, our detailed modeling is based on well-founded energy and mass balance equations and material properties, all of which individually have been experimentally confirmed. In addition, no new technologies are required for the electro-adsorption chiller: it should be manufacturable from existing elements.

Appendix. Detailed modelling equations

Definitions and reference values for the parameters and variables below are provided in Table 1.

Thermoelectric

The transient one-dimensional energy balance equation for a well-insulated thermoelectric couple of constant cross-section area A_{TE} and length L as a function of time t and position x ($0 \leqslant x \leqslant L$) is well approximated by [3]:

$$\frac{\partial T_{TE}(x,t)}{\partial t} = \frac{\lambda}{\rho_{dens} c_{TE}} \frac{\partial^2 T_{TE}(x,t)}{\partial x^2} + \frac{\rho_{elec} I^2}{A_{TE}^2 \rho_{dens} c_{TE}}. \quad \text{(A1)}$$

The equations for the power input for an array of N identical couples operated at constant voltage V, with time-responsive current $I(t)$, are [3]:

$$P_{in} = NVI(t) \quad \text{(A2)}$$

$$I(t) = \frac{-N\lambda A_{TE}\left[\left(\frac{\partial T_{TE}(x,t)}{\partial x}\right)_{x=0} + \left(\frac{\partial T_{TE}(x,t)}{\partial x}\right)_{x=L}\right] + N\int_0^L \rho_{dens} c_{TE} A_{TE}\left(\frac{\partial T_{TE}(x,t)}{\partial t}\right) dx}{N[V - \alpha(T_H - T_L)]}. \quad \text{(A3)}$$

Adsorber and desorber

The transient energy balance of the sorption beds accounts for (1) heat conduction at the interface with the thermoelectric; (2) sensible heating of the silica gel, water and heat exchanger; (3) the isosteric heat of adsorption; (4) heat generation or removal due to sorption; (5) heat input due to the thermoelectric Seebeck effect; (6) heat regeneration; and (7) switching control:

$$\left(M_{sg} c_{sg} + M_{hx} c_{hx} + (Mc)_{connect}\right)\frac{dT_{bed,i}}{dt} + M_{sg} q_{bed,i} \frac{dh_{bed,i}}{dt} - \sigma M_{sg} \frac{dq_{bed,i}}{dt}\left[\Delta H_{ads} + \delta\left(h_g(T_k) - h_g(p_k, T_{bed,i})\right)\right] = \pm\alpha I(t) T_{junc} \pm N\lambda A_{TE}\left(\frac{-\partial T_{TE}(x,t)}{\partial x}\right)_{junc} \quad \text{(A4)}$$

where h = specific enthalpy; $h_{bed} \approx h_g\left(p\left(q_{bed}, T_{bed,i}\right), T_{bed,i}\right) - \Delta H_{ads}$; subscripts $_g$ and $_{hx}$ denote the gas phase and sorption heat exchanger, respectively; and the controls correspond to

Operating stage	Sorption bed i	Switch control δ	Switch control σ	Subscript k	Sign in $\pm$	T_{junc}
Adsorption	Adsorber	1 if $dq_{bed}/dt \geqslant 0$, and 0 otherwise	1	Evaporator	−	T_L
Switching	(Desorber-to-be)	–	0	–	+	T_H
Desorption	Desorber	0 if $dq_{bed}/dt \leqslant 0$, and 1 otherwise	1	Condenser	+	T_H
Switching	(Adsorber-to-be)	–	0	–	−	T_L

The cycle-average values of Q_L and Q_H are calculated from the integration of Eq. (A4) over a single half-cycle.

Condenser and evaporator

The corresponding energy balance equations include (1) sensible heat transfer from both the condensate and adsorbate; (2) heat generation by condensation; (3) heat transfer to coolant air (condenser) or to the cooling load (evaporator); and (4) switching control. For a condenser cooled with air at temperature T_{air}, [6]

$$\begin{aligned}&\left[(Mc)_{cond}+M_{cond}^{refr}c_{cond}^{refr}(T_{cond})\right]\frac{dT_{cond}}{dt}\\&-\sigma\gamma h_f(T_{cond})M_{sg}\frac{dq_{des}}{dt}=\sigma M_{sg}\frac{dq_{des}}{dt}\times\\&\left[\delta(1-\gamma)h_f(T_{cond})-\delta h_g(T_{cond},p_{cond})-(1-\delta)h_g(T_{cond})\right]\\&-(UA)_{cond}(T_{cond}-T_{air})\end{aligned}\tag{A5}$$

where subscript $_f$ denotes the fluid phase; superscript ^{refr} denotes refrigerant; the temperature dependence of the refrigerant's (water's) specific heat is accounted for; and the overflow control γ is zero when the heat-exchange surface area on the vapor side of the condenser is saturated with condensate while $dq_{des}/dt \leqslant 0$, and unity otherwise [6]. Since the pressures and temperatures change in tandem, the adsorbent-adsorbate system follows an isosteric thermodynamic path.

For the evaporator [6]

$$\begin{aligned}&\left[(Mc)_{evap}+M_{evap}^{refr}c_{evap}^{refr}(T_{evap})\right]\frac{dT_{evap}}{dt}+\sigma h_f(T_{evap})\\&\frac{dM_{evap}^{refr}}{dt}=-\sigma\left\{(1-\delta)(1-\gamma)h_f(T_{cond})M_{sg}\frac{dq_{des}}{dt}\right.\\&\left.+M_{sg}\frac{dq_{ads}}{dt}\left[(1-\delta)h_g(T_{ads},p_{evap})+\delta h_g(T_{evap})\right]\right\}\\&-(UA)_{evap}(T_{evap}-T_{load})\end{aligned}\tag{A6}$$

where

$$\frac{dM_{evap}^{refr}}{dt}=M_{sg}\left[(1-\delta)(1-\gamma)\frac{dq_{des}}{dt}-\frac{dq_{ads}}{dt}\right].\tag{A7}$$

The dependence of the rate of heat transfer in nucleate pool boiling on the physical properties of the refrigerant and coolant, as well as on temperature and pressure, is taken from [12].

References

[1] Gordon JM, Ng KC. Cool thermodynamics. Cambridge: Cambridge International Science Publishing; 2000.

[2] Drost K, Friedrich M, Martin MC, Martin J, Hanna B. Mesoscopic heat-actuated heat pump development. ASME IMECE Conf. Nashville (TN): ASME, 1999.

[3] Rowe DM. CRC handbook of thermoelectrics. Boca Raton, FL: CRC Press LLC; 1995.

[4] Tritt TM. Holey and unholey semiconductors. Science 1999;283:804–5.

[5] DiSalvo F. Thermoelectric cooling and power generation. Science 1999;285:703–6.

[6] Chua HT, Ng KC, Malek A, Kashiwagi T, Akisawa A, Saha BB. Modeling the performance of two-bed, silica gel-water adsorption chillers. Int J Refrig 1999;22:194–204.

[7] Gordon JM, Ng KC, Chua HT, Chakraborty A. An electro-adsorption chiller: a miniaturized cooling cycle with applications from microelectronics to conventional air-conditioning. Patent pending; 2001.

[8] Yuan L, Joshi YK, Nakayama W. Effect of condenser location and imposed circulation on the performance of a compact two-phase thermosyphon. Engineering Foundation Conf. On Heat Transfer and Transport Phenomena for Microsystems. Banff, Canada: United Engineering Foundation Inc; 2000.

[9] Chen PH, Chen WC, Chang SH. Bubble growth and ink ejection process of a thermal ink jet printhead. Int J Mech Sci 1997;39:683–95.

[10] Lee DY, Vafai K. Comparative analysis of jet impingement and microchannel cooling for high heat flux application. Int J Heat Mass Transfer 1999;42:1555–68.

[11] Allen RR, Meyer JD, Knight WR. Thermodynamics and hydrodynamics of thermal ink jets. Hewlett-Packard Journal 1985;May:21–7.

[12] Rohsenow WM. A method of correlating heat transfer data for surface boiling liquids. Trans ASME 1952;74:969–75.